Adenosine Di- and Triphosphate Transport in Mitochondria. Role of the Amidine Region for Substrate Binding and Transport†

Eckhard Schlimme,* Karl-Siegfried Boos, and Egon Jabbo de Groot

ABSTRACT: A variety of base-modified nucleotide analogues was prepared and characterized as their α-^{32}P- or U-^{14}C-labeled compounds. Carrier-linked nucleotide binding and carrier-catalyzed exchange across the inner membrane of rat liver mitochondria were measured by using an inhibitor (atractyloside) stop method. Kinetic data of carrier-specific bound analogues were evaluated from Dixon plots and indicate that these analogues are competitive inhibitors for mitochondrial [^{14}C]ADP uptake. K_m and V_{max} values for carrier-mediated uptake of nucleotide analogues were calculated from Lineweaver–Burk plots. By means of the analogues, a systematic mapping of the essential chemical and steric interactions between the transporter protein and the heterocycle of its substrate in the course of the binding as well as transfer step was achieved. Prerequisites for carrier-specific binding (recognition) are (A) an anti- or syn-positioned β-glycosyl-linked heterocycle, (B) a nitrogen ring atom in position 7 for syn-structured analogues, and (C) an electron-rich region at the N(1) position, i.e., a permanent dipole moment oriented toward N(1) for anti-structured analogues. Additional requirements for subsequent transport catalysis are (A) a non-fixed anti-positioned base moiety with a β-glycosyl torsion angle of about −20°, (B) a C(6)-positioned amino group, and (C) an unsubstituted C(2) atom. The complementary binding site at the carrier protein to the N(1)–C(6)(–NH_2) amidine region is proposed to be represented by two juxtaposed and invariant bonding points, i.e., an asparagine or glutamine residue.

Analysis of the binding properties of structural analogues of a substrate provides an excellent approach to delineate the basic structures and modes of interaction which must participate in enzyme–substrate relations (Yount, 1975).

Our interest is directed to the carrier-mediated transfer of ADP and ATP across the inner mitochondrial membrane representing a key process of cellular energy supply. In this context, studies with chemically modified adenine nucleotide (ANP)[1] analogues should permit assignment of the binding points of the substrate in topography, polarity, charge, and solvation, thereby leading to a direct insight into the molecular mechanism of ANP translocation. Moreover, it should be possible to prove experimentally the two-step nature of the process, i.e., recognition and subsequent transfer by means of analogues, which are bound but not transported by the carrier protein.

Recently, translocation experiments carried out with a selected series of ribose-modified ANP analogues (Boos & Schlimme, 1979) provided a detailed description of the basic steric, contact, and structural elements which are prerequisites for carrier-specific binding and additionally for subsequent transport. In continuation of our previous studies (Schlimme & Schäfer, 1972; Schlimme & Stahl, 1974; Schlimme et al., 1977, 1979a,b), we investigated the binding and translocation properties of a series of base-modified nucleotides, as the hydrophobic moiety of the substrate molecule turned out to be of particular importance for transport catalysis.

Experimental Procedures

Materials. [U-^{14}C]ATP (196 mCi/mmol), [U-^{14}C]inosine (250 mCi/mmol), [U-^{14}C]guanosine (500 mCi/mmol), and [^{32}P]phosphorus oxychloride (1–50 mCi/mmol) were purchased from Amersham and NEN Chemicals. N^1-Methyl-, N^6-methyl-, and N^6,N^6-dimethyladenosines, nebularine, and tubercidin were products of Sigma-Chemie. Formycin A was obtained from Calbiochem.

Chemical Syntheses. N^1-Amino-INP (**7**) and N^1-amino-GNP (**8**) were prepared in the micromolar range from U-^{14}C-labeled INP and GNP, respectively, by reaction with hydroxylamine-*O*-sulfonic acid in 1 M NaOH at room temperature for 48 h as described for the appropriate nucleosides (Broom & Robins, 1969). N^1-Oxido-ANP (**5**) was prepared from U-^{14}C-labeled ANP by N(1)-oxidation with monoperphthalic acid (von der Haar et al., 1971). Triazoloinosine (**9**) was synthesized from [U-^{14}C]guanosine via N(1)-amination followed by cyclization in formamide at 180 °C for 45 min (Schlimme, 1978). 2-Aminoadenosine (**4**) and 2-aminonebularine (**3**) were prepared by Rackwitz & Scheit (1974).

The nucleoside analogues **1**, **2**, **3**, **4**, **10**, **11**, and **12** were chemically phosphorylated to the corresponding 5′-monophosphates by using [^{32}P]phosphorus oxychloride in either acetonitrile (Sowa & Ouchi, 1975) or trimethyl phosphate (Yoshikawa et al., 1967), respectively. The α-^{32}P-labeled nucleoside 5′-triphosphates were prepared via the phosphorylimidazolide (Cramer et al., 1961) according to Hoard & Ott (1965) in a modified procedure (Boos & Schlimme, 1979). Separation of the products from the reaction mixture was achieved by DEAE 52-cellulose column chromatography with a linear triethylammonium hydrogen carbonate gradient (Boos & Schlimme, 1979). N^1-Methyl-ANP (**6**) was prepared as an unlabeled compound and was purified by CM 52-cellulose column chromatography using ammonium formate (0–0.5 M, pH 2.6). For the enzymatic preparation and characterization of the corresponding nucleoside 5′-diphosphates, see Boos et al. (1976) and Schlimme et al. (1979a).

† From the Laboratorium für Biologische Chemie der Universität Paderborn, D-4790 Paderborn, Federal Republic of Germany. *Received March 19, 1980.* This study has been supported by grants from the Deutsche Forschungsgemeinschaft, the government of Nordrhein-Westfalen, and the Fonds des Verbandes der chemischen Industrie.

[1] Abbreviations used: ANP, adenine nucleotide (ADP, ATP); NeNP, nebularine di- or triphosphate; FNP, formycin di- or triphosphate; TuNP, tubercidin di- or triphosphate; triazolo-INP, 9-β-ribofuranosyl-*s*-triazolo[1,2-*a*]purin-6-one di- or triphosphate; GNP, guanosine di- or triphosphate; INP, inosine di- or triphosphate; Ap_5A, P^1,P^5-di(adenosine-5′) pentaphosphate.

0006-2960/80/0419-5569$01.00/0

Table I: Spectroscopic Properties of Base-Modified Adenine Nucleotides 1-12

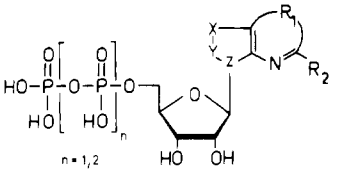

compd	no.	R_1	R_2	X–Y–Z	λ_{max} (nm)	ϵ (cm^2 μmol^{-1})
N^6-methyl-ANP	1	-C(NHCH$_3$)=N-	H	N=CH–N	266	15.9[a]
N^6-dimethyl-ANP	2	-C(N(CH$_3$)$_2$)=N-	H	N=CH–N	275	18.3[a]
2-amino-NeNP	3	-CH=N-	NH_2	N=CH–N	305	6.3[a]
2-amino-ANP	4	-C(NH_2)=N-	NH_2	N=CH–N	280	10.0[a]
					255	9.0
N^1-oxido-ANP	5	-C(NH_2)=N(→O)-	H	N=CH–N	259	9.3[a]
					232	40.6
N^1-methyl-ANP	6	-C(NH_2)=N$^+$(CH$_3$)-	H	N=CH–N	258	13.9[a]
N^1-amino-INP	7	-CON(NH_2)-	H	N=CH–N	251	9.9[b]
N^1-amino-GNP	8	-CON(NH_2)-	NH_2	N=CH–N	254	13.6[b]
triazolo-INP	9	-CON(R_2)-	NHCH=N	N=CH–N	285	14.3[b]
NeNP	10	-CH=N-	H	N=CH–N	262	5.9[a]
FNP	11	-C(NH_2)=N-	H	NH–N=C	295	10.7[a]
TuNP	12	-C(NH_2)=N-	H	CH=CH–N	270	12.1[b]

[a] Aqueous solution pH 7.0. [b] Aqueous solution pH 11.0.

Analytical Procedures. Mitochondrial protein was determined by the biuret method. Purity of the analogues was controlled by TLC (thin-layer chromatography) and LC (high-pressure liquid chromatography) according to Stahl et al. (1973). Radioactivity was measured with a liquid scintillation counter (Packard Tricarb 544) by using Aquasol (NEN Chemicals). Absorbance scans were recorded on a Shimadzu UV-200 spectrophotometer.

Total phosphate analysis was done according to Zilversmit & Davis (1950). The phosphorylation at the 5′ position was controlled by periodate oxidation of the 2′,3′-*cis*-diol group and subsequent TLC analysis. The phosphate moiety was further identified by ^{31}P NMR spectroscopy (Bruker WP 60 DS, 60 MHz). For the triphosphates the resonances centered at δ −6 (d, J = 20 Hz) for P(3), δ −21 (t, J = 19 Hz) for P(2), and δ −11 (d, J = 20 Hz) for P(1), whereas the corresponding diphosphates yielded δ −6 (d, J = 20 Hz) for P(2) and δ −11 (d, J = 20 Hz) for P(1) upfield to 85% H_3PO_4 as the external standard.

Translocation Measurements. Mitochondria were prepared from rat liver (male Wistar rats; 150–200 g weight) (Hagihara, 1950). Mitochondrial adenine nucleotide translocation studies were carried out at 5 °C by using the inhibitor stop method described by Pfaff & Klingenberg (1968). For further details in assaying, see Boos & Schlimme (1979). In inhibition experiments, sampling for rate measurements was performed within the linear phase (4–15 s) of [^{14}C]adenine nucleotide uptake at 5 °C under varying substrate concentrations ($\ll K_m$) according to Boos et al. (1975).

Results

Syntheses. Tables I and II summarize the analytical data of the investigated analogues.

Mitochondrial Binding and Exchange of Base-Modified Adenine Nucleotides. The capacity of rat liver mitochondria for carrier-linked (specific) binding and carrier-mediated exchange across the inner mitochondrial membrane as well as the amount of noncarrier-linked (unspecific) binding of ANP and the analogues was determined by means of the atractyloside-differentiation technique.

Saturation of the carrier-specific binding sites is achieved at an external [U-^{14}C]ANP concentration of 250 μM with 1.6 ± 0.2 nmol/mg of mitochondrial protein, whereas unspecific binding amounts to 0.6 ± 0.1 nmol/mg of mitochondrial protein. The exchange of ANP with the endogenous mitochondrial pool totals 1.7 ± 0.2 nmol/mg of mitochondrial protein under equilibrium conditions at 5 °C (see Table III).

Analogues derived from a lactam-type heterocycle, i.e., N^1-amino-INP (**7**) and N^1-amino-GNP (**8**), show no substrate properties. This behavior applies to the cyclicized compound triazolo-INP (**9**) as well. However, the structural isomer of

Table II: Chromatographic Properties of Investigated Analogues 1-12

	R_f values[a]				R_t values (min)[b]	
	A				D	
compd	n = 1	n = 2	B	C	n = 1	n = 2
1	0.60	0.32	0.72		31	82
2	0.61	0.27	0.81		26	70
3	0.53	0.29	0.62		22	56
4	0.40	0.16	0.36		46	95
5	0.61	0.47	0.43		38	114
6		[c]	0.60			
7	0.67	0.36	0.47		49	180
8	0.54	0.26	0.42		37	104
9	0.32	0.14	0.33		93	324
10	0.53	0.25		0.63	46	51
11	0.46	0.26		0.51	17	36
12	0.44	0.23		0.59	18	42

[a] TLC systems: (A) Polygram CEL 300 PEI/UV thin-layer plates (Macherey & Nagel, Darmstadt, Germany) with 0.75 M KH_2PO_4, pH 4.1, as the mobile phase; reference standards, ADP = 0.51, ATP = 0.23; 5′-diphosphate, n = 1; 5′-triphosphate, n = 2. (B) Cellulose F 1440 LS 254 thin-layer plates (Schleicher & Schüll, Dassel, Germany) with ethanol/1 M ammonium acetate (7:3 v/v) as the mobile phase for nucleosides; reference standard, adenosine = 0.57. (C) As in (B) except cellulose G 1440 plates; reference standard, adenosine = 0.49. The R_f values for nucleosides correspond to those obtained with authentic samples. [b] LC system: (D) column, 300 × 5 mm; flux rate, 9 mL/h; 33 bar; 24 °C; stationary phase, Nucleosil 10 SB (Macherey & Nagel, Düren, Germany); mobile phase, 0.3 M $LiNO_3$ and 0.02 M KH_2PO_4, pH 2.7; reference standards, AMP = 12.0, ADP = 22.0, and ATP = 58.5. [c] Electrophoresis (Desaga, Germany) on thin-layer plates (Silica gel F 254, ICN Woelm, Germany) in 0.1 M sodium citrate, pH 6.8, for 60 min at 400 V and 2 °C yielded the following mobilities: adenosine −0.3, AMP +1, ATP +1.7, N^1-methyladenosine +1.1, N^1-methyl-AMP +0.1, N^1-methyl-ATP +0.6.

Table III: Binding Properties of Base-Modified U-^{14}C- or α-^{32}P-Labeled Nucleotide Analogues to the Mitochondrial Adenine Nucleotide Carrier System

	properties [nmol/mg mitochondrial protein][a]		
compd	specific binding	exchange	unspecific binding
1	0.20 ± 0.14[b]	-[c]	0.35 ± 0.26
2	-	-	0.43 ± 0.29
3	0.50 ± 0.30	-	1.37 ± 0.46
4	1.00 ± 0.42	-	3.50 ± 1.17
5	0.70 ± 0.36	0.60 ± 0.31	0.75 ± 0.29
7	-	-	1.10 ± 0.42
8	-	-	1.50 ± 0.67
9	-	-	0.92 ± 0.47
10	0.41 ± 0.08	-	0.73 ± 0.18
11	1.33 ± 0.40	1.30 ± 0.20	0.68 ± 0.12
12	2.20 ± 0.20	0.69 ± 0.22	2.28 ± 0.07

[a] The extramitochondrial nucleotide analogue concentration was varied in a range up to 250 μM. The values reported were taken at saturation condition for ANP, i.e., 250 μM at 5 °C. Due to the fact that during the incubation phosphoryl transfer reactions take place, even in the presence of oligomycin and Ap_5A, all experimental findings are expressed as ANP instead of the appropriate nucleoside triphosphates added at the beginning of the translocation experiments. [b] Calculation of error ranges. The range of confidence (95%) for the individual experimental values obtained by the atractyloside-differentiation method, i.e., (A) specific binding + unspecific binding + exchange, (B) unspecific binding, and (C) unspecific binding + exchange, was calculated. Subtraction, i.e., calculation of the binding (A–C)–as well as the exchange (C–B)–data was carried out only if the confidence ranges (95%) did not overlap. The mean values thus obtained from four independent experiments were used to calculate the range of confidence (95%) for the data presented. [c] Dashes indicate no significant binding or exchange within the range of confidence of 95%.

N^1-amino-INP, i.e., N^1-oxido-ANP (**5**), is specifically bound and transported across the inner membrane. The structural integrity of the transported N^1-oxido analogue was established by radiochromatographic analysis (cf. Figure 1a,b). From the data presented it is obvious that this derivative is not reduced in situ to ANP.

In the case of N^1-methyl-ANP (**6**), the application of the atractyloside-differentiation technique failed. This might be due to chemical interaction with mitochondria (cf. Discussion) as acidic extraction and subsequent TLC analysis of the translocation assay did not reveal quantitatively the analogue or its rearranged product (**1**). Introduction of one methyl group at the C(6) amino group (**1**) markedly reduces carrier-specific binding. Dimethylation of the exocyclic substituent (**2**), on the other hand, results in a total loss of specific binding properties. Deamination at the C(6) position and/or introduction of an amino group at the C(2) position gives rise to analogues, i.e., **3**, **4**, and **10**, which still show carrier-specific binding but no transport activity. The modification of the imidazole ring system by substitution of the heteroatoms, as in FNP (**11**) and TuNP (**12**), is tolerated by the carrier system. This is further substantiated by the fact that FNP (**11**) and TuNP (**12**) induce a state 3/state 4 respiration in oxidative phosphorylation of rat liver mitochondria (K. S. Boos and E. Schlimme, unpublished results).

Effect of Substrate Analogues on the Uptake of [U-^{14}C]-ANP by Rat Liver Mitochondria. Sampling for rate measurements was performed within the first 4–15 s of [U-^{14}C]-ANP uptake (Boos & Schlimme, 1979). Competition studies were carried out with analogues which were found to bind specifically to the carrier protein, i.e., **1**, **3**, **4**, and **10**, or those showing distinct unspecific binding, i.e., **9**.

All the analogues studied in the inhibition experiments (cf. Table IV) inhibit the [U-^{14}C]ANP uptake competitively. The K_I values have about the same order of magnitude as K_m of

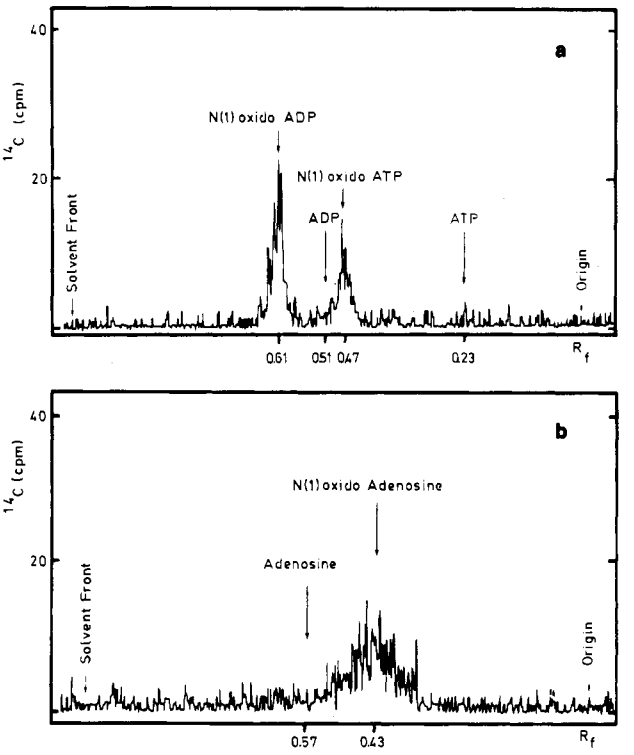

FIGURE 1: Radiochromatography of the N^1-oxido derivative after mitochondrial translocation. (a) Mitochondria were incubated for 2 min (Boos et al., 1975) with N^1-oxido[^{14}C]ATP (250 μM; 2.45 × 10^6 cpm/μmol), and translocation was terminated by centrifugation through a silicone oil layer. The pellet (1 mg of mitochondrial protein) was resuspended in water and analyzed by TLC using system A (see Table II). ADP and ATP were run in parallel and detected by UV absorption. Subsequent scanning by a TLC linear detector (Berthold, Germany) yielded, besides N^1-oxido[^{14}C]ATP, its diphosphate as the degradation product. (b) An aliquot of the resuspended pellet (see Figure 1a) was treated with alkaline phosphatase (see Methods and Materials) and analyzed by TLC using system B (see Table II). Adenosine was run in parallel and detected by UV absorption. N^1-Oxidoadenosine was identified by TLC scanning as the only ^{14}C-labeled degradation product.

Table IV: Kinetic Parameters of Substrate Analogues in Mitochondrial ANP Transport

compd[a]	K_m (μM)[b]	K_I (μM)[b]	V_{max} [nmol min^{-1} (mg of protein)$^{-1}$]
1	-	190 (100–240)[c]	*d*
3	-	290 (140–440)	*d*
4	-	155 (90–210)	*d*
5	530 (470–605)	-	13.70 (7.00–24.50)
9	-	≥1000	*d*
10	-	54 (6–88)	*d*
11	100 (25–275)	-	6.75 (4.30–16.40)
12	110 (70–240)	-	9.10 (6.00–18.50)

[a] Initial addition of the corresponding triphosphates; see also Table II, footnote *a*. [b] Inhibition constants (K_I) and maximum velocities (V_{max}) for [U-^{14}C]ANP uptake were derived from Dixon plots. Michaelis-Menten constants K_m and V_{max} for carrier-mediated uptake were calculated from Lineweaver-Burk plots. [c] Numbers in parentheses indicate the range of confidence (95%) for graphic determination (Stahl et al., 1974). [d] V_{max} values evaluated from Dixon plots were in the confidence range (95%) for the noninhibited [U-^{14}C]ANP uptake.

ANP = 41 (29–83) μM (Boos et al., 1975). The competitive inhibitory nature is furthermore substantiated by the fact that V_{max} of [U-^{14}C]ANP uptake [7.0 (5.7–9.1) nmol min^{-1} (mg of protein)$^{-1}$ (Boos et al., 1975)] is not affected significantly under the presence of substrate analogues. The "competitive" nature of triazolo-INP (**9**) may be interpreted as previously

for highly lipophilic analogues (Boos & Schlimme, 1979). The K_m and V_{max} values for transmembrane exchange of FNP (**11**) and TuNP (**12**) are in the same order of magnitude as for ANP. N^1-Oxido-ANP (**5**) shows a 5 times lower affinity to the transporter protein.

Discussion

This study with a series of base-modified analogues confirms the remarkable specificity displayed by the ANP carrier protein for recognition and transport catalysis of its substrates. Analysis of the binding results permits the assignment of basic specificity elements involved as well as a more detailed interpretation of the mode of substrate binding and transfer.

None of the naturally occurring ribo- or deoxyribonucleoside 5′-*O*-tri(di)phosphates of pyrimidine derivatives, i.e., uracil, thymine, and cytosine, exhibit carrier-specific binding. Substitution of the C(6)-positioned amino group of the natural substrate by an oxygen atom, as in the purine derivatives inosine and guanosine, or dimethylation of the C(6)–NH_2 group impedes specific binding to the carrier protein as well. The same effect is observed after the introduction of an amino group at the N(1) position of lactam-type purine nucleotides as in **7** and **8** or after cyclization as in triazolo-INP (**9**).

On the other hand, specific binding properties are retained after deamination of the natural substrate at the C(6) position as in **10** and/or C(2) amination as in **3** and **4**. N(1)-Oxidation is the only chemical modification of the purine moiety known so far which preserves translocation properties. The affinity, however, is reduced to about one order of magnitude compared with the natural compound. This might explain the results of Mantsch et al. (1975), who used a non-radioactive-labeled analogue in their transport studies. N^1-Amino-INP (**7**), the structural isomer of **5**, is not a substrate either for carrier-linked binding or for exchange. These findings conclusively point out the requirement of a C(6)-positioned NH_2 group and an unsubstituted C(2) atom for transport catalysis, thereby excluding any guanine-like structure. As far as the imidazole ring system is concerned, substitution of the heteroatoms by carbon atoms as in FNP (**11**) and TuNP (**12**) gives rise to analogues which show K_m and V_{max} values comparable to ANP. Recently, our results with FNP (**11**) were confirmed by fluorescence measurements by Graue & Klingenberg (1979). N^1-Methyl-ANP (**6**) very probably is covalently linked to the membrane and/or carrier protein by a Dimroth rearrangement upon nucleophilic attack.

Besides the findings concerning the influence and importance of the exocyclic substituents and ring atoms at the purine moiety on the interaction with the transport system, the results obtained allow a detailed description of the basic steric factors involved in substrate binding and transport. A major structural parameter of nucleotide conformation is the rotation of the planar heterocycle around the glycosyl bond. The torsion angle ϕ_{CN} given by the projections O(1′)–C(1′) and N(9)–C(8) is defined to $-30 \pm 45°$ for an anti conformation and to $150 \pm 45°$ for a syn orientation (Sundaralingam, 1969; Ts'o, 1974). CPK model studies revealed that the N(1)–C(6)(–NH_2) amidine region of anti-structured nucleotides overlaps with the N(7)–C(5)–C(6)(–NH_2) system of syn-type analogues. N(7) thus might substitute for N(1) in carrier-specific binding of syn-structured analogues. Transmembrane exchange, however, primarily depends on a nonfixed β-linked nucleobase within narrow confines of the anti region with ϕ_{CN} approximately −20° (Schlimme & Stahl, 1974; Boos et al., 1978; Schlimme et al., 1977; Boos & Schlimme, 1979).

This is in line with the results presented here. N^1-Oxido-ANP (**5**) and TuNP (**12**) are anti-structured nucleotide analogues. Because of repulsive electrostatic interactions between N(8) and the ribose oxygen O(5′), FNP (**11**) is known to exhibit a "high-anti" conformation, i.e., the heterocycle is centered in the syn/anti boundary region with $\phi_{CC} = -109°$. However, due to the increased glycosyl bond length and the loss of the steric hindrance of H(8), the rotational energy barrier is lowered. FNP thus can adopt an anti conformation possessed by the natural substrate (Sundaralingam, 1975).

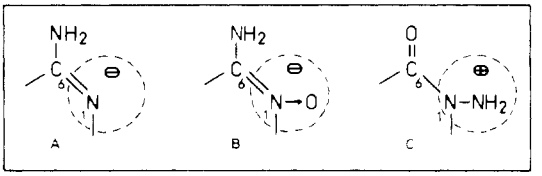

FIGURE 2: π-Electron charge distribution in the N(1)–C(6)(–NH_2) amidine region: (A) adenine; (B) N^1-oxidoadenine; (C) N^1-aminoinosine. A charge deficiency is indicated as a circled plus and an excess as a circled minus sign.

In this context, nucleotide–metal complexation cannot be excluded for specific binding as it is known that anti- and syn-structured nucleotides can coordinate with N(7) and N(1), respectively. Translocation experiments with exchange-inert Co(III) and Cr(III) ANP complexes (K. S. Boos and E. Schlimme, unpublished results) support this assumption. The findings with anti-structured 7-deaza-ANP (TuNP, **12**), syn-structured 8-bromo-ANP (Schlimme & Stahl, 1974), and conformationally restricted ANP analogues (Boos et al., 1978) suggest no metal–nucleotide interaction in the course of the transfer step.

In addition to its size and orientation, the π-electron charge distribution of the purine base obviously contributes to binding. As already pointed out above, the purine derivatives inosine and guanosine are not recognized by the carrier protein. These findings and the presented results suggest that for specific binding an electron-rich region at the N(1) purine position, indicated by a circled minus sign in Figure 2, is necessary and sufficient (Schlimme et al., 1979b). This π-electron charge distribution is at least qualitatively realized in N^1-oxido-ANP (Figure 2B) but not in its isomeric compound N^1-amino-INP (Figure 2C).

It was shown that a nucleobase exhibits a permanent dipole moment whose magnitude and direction depend on the substituents at the ring system as well as on the orientation of the heterocycle with respect to the ribose moiety (Berthod & Pullman, 1972; Ts'o, 1974; Vetterl, 1976). The dipole moment is oriented with its negative end toward the N(1) atom in adenine, N(7) in lactam-type derivatives, and C(2) in pyrimidines.

These observations correlate with the π-electron charge distribution in the amidine region (cf. Figure 2). The failure of lactam-type analogues, i.e., **7**, **8**, **9**, guanosine, and inosine as well as of pyrimidines, i.e., cytosine, uracil, and thymine, to bind to the carrier protein may be due to the wrong orientation of their permanent dipole moment. The prerequisites of a π-electron charge accumulation at N(1) for substrate recognition and in addition a C(6)–NH_2 group for transport catalysis imply that an invariant region must be present at the nucleobase binding domain. The invariance becomes obvious by the binding properties of N^1-amino-INP (**7**). The complementary binding sites are proposed to be represented by a hydrogen-accepting and -donating asparagine or glutamine residue (cf. Figure 3).

Previous studies (Boos & Schlimme, 1979) indicated a decisive functional importance of the trans-positioned C(2′) hydroxyl group. Upon binding, a specifically spaced hydro-

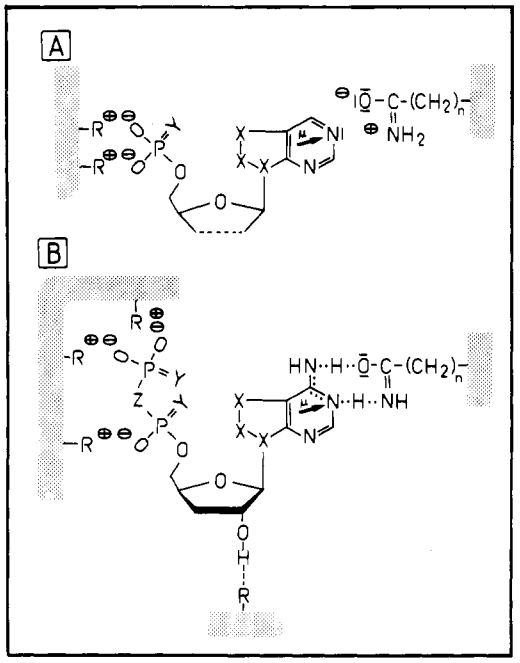

FIGURE 3: Schematic representation of the molecular requirements for the substrate binding (recognition) (A) and transport step (B). The invariant nucleobase binding site at the carrier protein is proposed to be an asparagine ($n = 1$) or glutamine ($n = 2$) residue. Amino acid analysis of the isolated ANP carrier protein (Aquila et al., 1978; Bojanovski et al., 1978) as well as of a peptide obtained by cyanogen bromide cleavage of the carrier protein after photolabeling with arylazidoatractyloside (Boulay et al., 1979) yielded the amino acids glutamate and aspartate. This is in line with our proposal as acidic hydrolysis generates the corresponding carboxylic derivatives. According to its predominant structure (Stewart & Siddall, 1970), the amide is drawn with a CN double bond. For specific binding, the N(1)–amide attraction is sufficient. The transfer step, however, requires the partition of the N(1)–C(6)($-NH_2$) amidine region, thereby inducing an amino $\rightleftharpoons$ imino tautomerism (indicated by dotted lines) which is proposed to be essential for catalysis. An arginine residue could be eliminated as a bonding site due to the pK_a value of its guanidine group. The resulting symmetric charge distribution of its functional side chain excludes the required invariance. R represents a hydrogen-accepting amino acid residue; broken lines indicate the H-bonding interaction. X corresponds to a nitrogen or carbon ring atom and Y to an oxygen or sulfur atom. Z indicates an oxygen or no bridge atom. μ denotes the permanent dipole moment whose direction is indicated by an arrow. Electrostatic interaction of a minimum of one to two negative charges presumably attaches the phosphate moiety in the course of the binding process to positively charged amino acid side chains indicated as R^+, whereby metal complexation cannot be excluded as well. For transport catalysis, however, at least three negative charges have to be present.

gen-accepting group at the carrier protein (cf. Figure 3) and/or partial desolvation of the hydrated ribose moiety leads to a stereospecific protein–ligand interaction which "triggers" the ANP transfer step. In addition, distinct purine-like distances between the amidine region and the ribose bearing five-membered ring must be fulfilled. This can be concluded from the nonbinding properties of a "stretched out" analogue, i.e., lin-benzo-ATP (Kauffman et al., 1978).

These sequential molecular events, i.e., recognition and transport catalysis, fit into the concept of a "gated pore" mechanism as the mode of mitochondrial ANP transport. Though the carrier protein recalls and senses by weak bonding interactions only a minimum structure, i.e., a 4-aminopyrimidine linked to the 5′-diphosphoribose moiety by a 6,1′ β-CH_2 or –NH– bridge, from the relatively complex information contents of the ANP molecule, this chemical communication between ligand and macromolecule ensures a remarkably high specificity. Moreover, on the basis of the postulated three-point attachment via the amidine region, the C(2′) ribose hydroxyl group, and the phosphate moiety, each of the functional and structural relevant nucleotide segments is involved and guarantees, in addition, specificity.

Acknowledgments

We thank Professor K. H. Scheit, MPI für Biophysikalische Chemie, Göttingen, Germany, for kindly supplying us with 2-aminoadenosine and 2-aminonebularine and Drs. W. Draber and W. Donner, Bayer AG, Leverkusen, Germany, for the calculation of the π-electron charge distribution.

References

Aquila, H., Eiermann, W., Babel, W., & Klingenberg, M. (1978) *Eur. J. Biochem. 85*, 549.

Berthod, H., & Pullman, B. (1972) *Biochem. Biophys. Res. Commun. 46*, 125.

Bojanovski, D., Schlimme, E., Bojanovski, M., Wang, C. S., Alaupovic, P., Folkhard, W., & Pilz, I. (1978) in *Protides of the Biological Fluids* (Peeters, H., Ed.) pp 37–41, Pergamon Press, Oxford and New York.

Boos, K. S., & Schlimme, E. (1979) *Biochemistry 18*, 5304.

Boos, K. S., Schlimme, E., Bojanovski, D., & Lamprecht, W. (1975) *Eur. J. Biochem. 60*, 451.

Boos, K. S., Lüstorff, J., Schlimme, E., Hesse, H., & Strotmann, H. (1976) *FEBS Lett. 71*, 124.

Boos, K. S., Schlimme, E., & Ikehara, M. (1978) *Z. Naturforsch. C: Biosci. 33C*, 552.

Boulay, F., Lauquin, G. J. M., & Vignais, P. V. (1979) *FEBS Lett. 108*, 390.

Broom, A. D., & Robins, R. K. (1969) *J. Org. Chem. 34*, 1025.

Cramer, F., Schaller, H., & Staab, H. A. (1961) *Chem. Ber. 94*, 1612.

Graue, C., & Klingenberg, M. (1979) *Biochim. Biophys. Acta 546*, 539.

Hagihara, B. (1950) *Biochim. Biophys. Acta 46*, 134.

Hoard, D. E., & Ott, D. G. (1965) *J. Am. Chem. Soc. 87*, 1785.

Kauffman, R. F., Lardy, H. A., Barrio, J. R., Barrio, M. C., & Leonard, N. J. (1978) *Biochemistry 17*, 3686.

Mantsch, H. H., Goia, J., Kezdi, M., Bârcu, O., Dânsoreanu, M., Jebeleanu, G., & Ty, N. G. (1975) *Biochemistry 14*, 5593.

Pfaff, E., & Klingenberg, M. (1968) *Eur. J. Biochem. 6*, 66.

Rackwitz, H. R., & Scheit, K. H. (1974) *Chem. Ber. 107*, 2284.

Schlimme, E. (1978) *Z. Naturforsch. C: Biosci. 33C*, 326.

Schlimme, E., & Schäfer, G. (1972) *FEBS Lett. 20*, 659.

Schlimme, E., & Stahl, K. W. (1974) *Hoppe-Seyler's Z. Physiol. Chem. 335*, 1139.

Schlimme, E., Boos, K. S., Bojanovski, D., & Lüstorff, J. (1977) *Angew. Chem., Int. Ed. Engl. 16*, 695.

Schlimme, E., de Groot, E. J., Schott, E., Strotmann, H., & Edelmann, K. (1979a) *FEBS Lett. 106*, 251.

Schlimme, E., Boos, K. S., & de Groot, E. J. (1979b) in *Molecular Mechanism in Biological Recognition* (Balaban, M., Ed.) pp 443–450, Elsevier/North-Holland Biomedical Press, Amsterdam.

Sowa, T., & Ouchi, S. (1975) *Bull. Chem. Soc. Jpn. 48*, 807.

Stahl, K. W., Schlimme, E., & Bojanovski, D. (1973) *J. Chromatogr. 83*, 395.

Stahl, K. W., Schlimme, E., & Eckstein, F. (1974) *FEBS Lett. 40*, 241.

Stewart, W. E., & Siddall, T. H., III (1970) *Chem. Rev. 70*, 517.

Sundaralingam, M. (1969) *Biopolymers 7*, 821.

Sundaralingam, M. (1975) *Ann. N.Y. Acad. Sci. 255*, 3.
Ts'o, P. O. P. (1974) *Basic Princ. Nucleic Acid Chem. 1*, 453–517.
Vetterl, V. (1976) *Bioelectrochem. Bioenerg. 3*, 338.
von der Haar, F., Schlimme, E., Erdmann, V. A., & Cramer, F. (1971) *Bioorg. Chem. 1*, 282.
Yoshikawa, M., Kato, T., & Takenishi, T. (1967) *Tetrahedron Lett. 50*, 5065.
Yount, R. G. (1975) *Adv. Enzymol. Relat. Areas Mol. Biol. 43*, 1.
Zilversmit, D. B., & Davis, A. K. (1950) *J. Lab. Clin. Med. 35*, 155.

Role of 2′,5′-Oligo(adenylic acid) Polymerase in the Degradation of Ribonucleic Acid Linked to Double-Stranded Ribonucleic Acid by Extracts of Interferon-Treated Cells†

Timothy W. Nilsen, Sanford G. Weissman, and Corrado Baglioni*

ABSTRACT: RNA covalently linked to double-stranded RNA (dsRNA) is preferentially degraded in extracts of interferon-treated HeLa cells [Nilsen, T. W., & Baglioni, C. (1979) *Proc. Natl. Acad. Sci. U.S.A. 76*, 2600–2604]. The size of the dsRNA required for this preferential degradation has been determined by annealing poly(I) of known length to the poly(C) tract of encephalomyocarditis virus (EMCV) RNA or by annealing poly(U) to poly(A) of known length of vesicular stomatitis virus mRNA. The dsRNA must be longer than about 60 base pairs to observe the preferential degradation of RNA. Moreover, triple-stranded regions that do not activate synthesis of 2′,5′-oligo(A) and ethidium bromide, which intercalates in dsRNA and blocks 2′,5′-oligo(A) polymerase activation, prevent this degradation. Ethidium also blocks the degradation of the replicative intermediate of EMCV by extracts of interferon-treated cells. These experiments indicate that synthesis of 2′,5′-oligo(A) is required for the degradation of RNA linked to dsRNA. The 2′,5′-oligo(A)-dependent endonuclease does not cleave single- or double-stranded DNA, nor does it cleave homopolyribonucleotides. The potential role of the 2′,5′-oligo(A) polymerase/endonuclease system in the inhibition of viral RNA replication is discussed.

Interferon induces in mammalian and avian cells an oligonucleotide polymerase; this enzyme can be activated in cell extracts by double-stranded RNA (dsRNA) and converts ATP into a series of oligonucleotides designated 2′,5′-oligo(A) (Kerr & Brown, 1978). The 2′,5′-oligo(A) activates an endonuclease that degrades mRNA (Baglioni et al., 1978; Clemens & Williams, 1978). This nuclease activity may play an important role among the antiviral defense mechanisms that inhibit the replication of RNA viruses in interferon-treated cells. This is suggested by the presence of 2′,5′-oligo(A) in cells treated with interferon and infected with encephalomyocarditis virus (EMCV) (Williams et al., 1979b) and by the inhibition of EMCV and vesicular stomatitis virus (VSV) replication upon introduction of 2′,5′-oligo(A) in mammalian cells (Williams et al., 1979a; Hovanessian & Wood, 1980). Both viral and cellular RNA appear to be degraded in the presence of 2′,5′-oligo(A) under these conditions (Hovanessian et al., 1979), whereas no significant degradation of cellular RNA can in general be detected in interferon-treated cells infected by viruses [reviewed by Stewart (1979)]. If the endonuclease is activated in intact cells, it therefore discriminates between cellular and viral RNA and preferentially degrades only the latter.

A mechanism for discrimination between cellular and viral RNA by the 2′,5′-oligo(A) polymerase/endonuclease system was proposed by Nilsen & Baglioni (1979a). In cells infected by viruses that replicate by forming structures containing dsRNA, the polymerase may bind to viral dsRNA, form limited amounts of 2′,5′-oligo(A), and activate the endonuclease at the site of viral RNA synthesis. Experiments with cell extracts provided experimental support for such a mechanism. Viral replicative intermediates and RNA covalently linked to dsRNA were preferentially degraded only in extracts of interferon-treated cells (Nilsen & Baglioni, 1979a). This degradation occurred only under incubation conditions that allowed synthesis of 2′,5′-oligo(A).

In the present study we investigated the structural features of dsRNA required to observe the preferential degradation of covalently linked RNA. These structural features are essentially identical with those required for the activation of 2′,5′-oligo(A) synthesis (Minks et al., 1979b). These experiments were carried out with RNAs containing base-paired regions of known compositions and length or with ethidium bromide that intercalates with dsRNA and inhibits activation of 2′,5′-oligo(A) polymerase (Baglioni & Maroney, 1980). Finally, by assaying the degradation of different substrates, we established that the 2′,5′-oligo(A)-dependent endonuclease does not cleave homopolyribonucleotides.

Experimental Procedures

Cell Extracts. HeLa S3 cells were grown in suspension in minimal essential medium supplemented with 5% calf serum. Cytoplasmic extracts were prepared from cells treated for 17 h with 100 units/mL of human fibroblast interferon (3×10^5 units/mg of protein; obtained from the Interferon Working Group of the National Cancer Institute, NIH) or from untreated cells as previously described by Baglioni et al. (1978).

Preparation of Labeled Viral RNA. Vesicular stomatitis virus (VSV) mRNA was synthesized by in vitro transcription with replicative complexes obtained from infected cells as previously described by Toneguzzo & Ghosh (1976). The

† From the Department of Biological Sciences, State University of New York at Albany, Albany, New York 12222. *Received April 22, 1980.* This work was supported by Grant AI 16076 from the National Institutes of Health.

0006-2960/80/0419-5574$01.00/0